Soft Matter

RSC Publishing

PAPER

View Article Online
View Journal | View Issue

Propagation of ultrasound in aqueous foams: bubble size dependence and resonance effects

Cite this: *Soft Matter*, 2013, **9**, 1194

Imen Ben Salem,[a] Reine-Marie Guillermic,†[a] Caitlin Sample,[a] Valentin Leroy,[b] Arnaud Saint-Jalmes[a] and Benjamin Dollet*[a]

We report experimental results on the propagation of ultrasonic waves (at frequencies in the range of 40 kHz) in aqueous foams. Monitoring the acoustics of the foams as they age, *i.e.* as the mean bubble radius increases by coarsening, we recover at short times some trends that are already known: decrease of the speed of sound and increase of attenuation. At long times, we have identified, for the first time, robust non-monotonic behaviors of the speed of sound and attenuation, associated with a critical bubble size, which decreases at increasing frequency. The experimental features appear to be surprisingly reminiscent of the Minnaert resonance known for a single isolated bubble in a fluid. Transposing the Minnaert theoretical framework to the limit of a dense packing of bubbles gives some qualitative agreement with the data, but still cannot explain quantitatively the measured properties.

Received 8th March 2012
Accepted 7th November 2012

DOI: 10.1039/c2sm25545f

www.rsc.org/softmatter

I Introduction

When dispersing a large amount of gas into a surfactant solution, one gets an aqueous foam, consisting of packed bubbles of gas embedded into a fluid network. The surfactants adsorbed at the gas–liquid interfaces provide repulsive forces, preventing the bubbles from coalescing. Together with the bubble radius a, the liquid fraction ϕ_ℓ (defined as the volume of liquid divided by the volume of foam) is an important physical parameter of a foam. This quantity describes the amount of compression of the bubbles: when ϕ_ℓ equals a few percent, bubbles become polyhedral by sharing thin planar facets. Due to this packing of bubbles a foam has very peculiar and striking features, intermediate between those of a fluid and a solid; for these reasons, they are widely used in various fields of applications.[1–3]

Among these specificities, an important one is that a foam ages, as a gas–liquid dispersion is an out-of-equilibrium system. A foam evolves in time by gravitational drainage, resulting in a decrease of the overall liquid fraction ϕ_ℓ, and by coarsening due to gas diffusion, resulting in an increase of the average bubble radius a.[3,4] Over the years, it has been shown that the dynamics and timescales of the aging process, as well as many foam features, depend strongly on the initial values of these two quantities a and ϕ_ℓ. Also, the chemical formulation plays a role by controlling the viscoelasticity of both the fluid and the bubble interfaces.

In practice, independent rheometric measurements can determine the bulk and interfacial viscoelasticity. This is less simple for a and ϕ_ℓ: they need to be measured to predict the behavior, characterize the foam and compare it with others. It is also important to determine whether or not the foam is initially uniform in terms of a and ϕ_ℓ. Then, one must be able to monitor how these quantities evolve in time and space. It turns out that these measurements remain a tricky task, and simple and reliable techniques providing these values and their distribution *in situ* as a function of time are still not known. Optically, as soon as the sample has about ten bubbles in thickness (for ϕ_ℓ typically of a few percent), it becomes tricky to visualize each bubble, and the foam becomes opaque. In fact, most of the foams produced or used are well into this limit of opacity: the incident light is multiply scattered, and the sample looks white. In this respect, foam is a good example of many other systems that diffuse light: emulsion, concentrated suspensions, clouds, *etc.* Nevertheless, it was shown that it is possible to take advantage of multiple scattering: techniques such as Diffuse Transmission Spectroscopy (DTS) and Diffusive Wave Spectroscopy (DWS) have been developed for turbid media,[5,7] and are well suited for foams.[6,8,9] Much information has been extracted by DWS on foams: on the time evolution of the bubble size, rate of coarsening-induced rearrangements, *etc.* However, these techniques only provide averaged values and as the foam scattering properties depend non-trivially on the liquid fraction and bubble size,[9] it is not possible to measure and separate these quantities by a single optical setup. To avoid multiple scattering of waves by the foam structure, X-rays were used: tomographic reconstruction has confirmed scaling behaviors

[a]*Institut de Physique de Rennes, UMR 6251 CNRS/Université Rennes 1, Campus Beaulieu, Bâtiment 11A, 35042 Rennes Cedex, France. E-mail: benjamin.dollet@univ-rennes1.fr*

[b]*Matière et Systèmes Complexes, UMR 7057 CNRS/Université Paris Diderot, 10 rue Alice Domon et Léonie Duquet, 75013 Paris, France*

† Present address: Department of Physics and Astronomy, University of Manitoba, Winnipeg, Manitoba R3T 2N2, Canada.

during coarsening,[10] but this approach requires expensive equipment or dedicated facilities like synchrotrons, and is limited by relatively long acquisition times. Measuring the foam electrical conductivity is indeed a simple and robust approach; such a measurement provides the local liquid fraction between two electrodes; it has been used for many years in the foam community,[11–13] and recently a complete calibration curve was obtained.[14] But, this method does not provide information about bubble sizes, nor on interfacial behavior.

In the same spirit of measuring the transport of optical and electrical signals through a foam, the propagation of acoustic signals can be another option. Many studies deal with the interaction of a single bubble with an acoustic wave, from the pioneering work of Minnaert on the existence of a bubble acoustic-induced resonance[15–17] to manipulation of a bubble by sound in microfluidic channels.[18,19] But shifting from this limit of a single drop or bubble to the opposite case of thousands of packed bubbles inside a foam is still challenging. In the intermediate range, there are results on very dilute bubbly liquids,[20,21] clouds of bubbles,[22–24] or 2D rafts of bubbles.[25] On macroscopic 3D foams, it turns out that there are only some studies,[26–34] mostly evidencing that sound is strongly attenuated and basically propagates at a speed as low as 50 m s^{-1} (about 7 times slower than in air) inside a foam of submillimetric bubbles. If this order of magnitude can be captured by considering that foam has the compressibility of the gas, with the density of the liquid (following the classical model of Wood[36]), the existing studies show that this picture is not sufficient.

Nevertheless, these results already show that foam acoustics deserve to be investigated if one wants to develop new diagnostics to macroscopically characterize a foam. Moreover, studying acoustic propagation in a foam has some fundamental aspects: understanding acoustic in a complex disordered random matrix remains difficult, and foams could be used as model systems, as their intrinsic properties like a and ϕ_ℓ can be widely tuned without changing the geometrical arrangement of the structure (dictated by the so-called "Plateau rules"[1–3]). It is also interesting to compare optical and acoustic scattering in such disordered media; in this respect, it has already been shown that techniques like DWS can be transposed to acoustic signals.[37,38] Also, as recently shown for 2D bubble rafts,[25] developments of meta-materials or phononic systems based on drops and bubbles can be considered;[39] clearly, this opens new routes which need first an understanding of sound propagation in many controlled bubble systems. Lastly, one can wonder whether acoustics could lead to *in situ* bulk or interfacial rheometry, at high frequencies and not accessible by other devices.[33]

In this article, we present new results on foam acoustics in the ultrasound range (at typically 40 kHz): we have monitored various acoustic properties as a function of bubble radius, at a quasi-constant liquid fraction. We show that non-trivial features are observed, which cannot be explained by the usual mean-field approach. In particular, the bubble size turns out to be a crucial parameter: the experimental features are consistent with an acoustic resonance at a critical value of this size. After presentation of the experimental details and data, we discuss in detail whether existing models can explain these results.

II Foams and acoustic methods

A Selection of the acoustic setup

To emit and receive sound, we selected two MA40E7R/S piezoelectric transducers, which have a resonance frequency of 40 kHz. We also chose a simple configuration: the transducers are placed face to face on a rail, allowing their distance d to be varied (Fig. 1a). The latter is measured with a caliper, with uncertainty estimated to be 50 μm at most. At the beginning of the experiment, the foam is simply injected between the two transducers, forming a heap, of typically 3 cm height, and stable due to its yield stress. The foam is thus not confined by side walls, while the small height is also useful for drainage issues (as discussed below).

An input signal is generated by a function generator (DS 345, Stanford Research Systems) and amplified by a power amplifier (WMA-300, Falco Systems), then sent to the emitting transducer. The electric signal recorded by the receiving transducer is recorded by an oscilloscope (DSO6014A, Agilent Technologies), then acquired on a computer *via* a home-made Labview program.

B Selection of the foam types and properties

The challenge is to determine how the foam acoustic properties depend on the foam physical properties, a and ϕ_ℓ. This implies that one must be able to tune separately these parameters in a controlled way, and to have independent measurements of them. Our strategy is to use the natural aging of the foam, together with an efficient choice of the initial foam parameters. It is known that the timescales of coarsening (which changes the bubble size) and drainage (which changes the liquid fraction) depend on the initial a and ϕ_ℓ. In the limits of tiny bubbles (a < 0.5 mm) and dry foams (ϕ_ℓ < 0.1), coarsening dominates drainage.[3,4] With such bubble sizes, drainage can even be almost suppressed, if samples have a height of a few centimeters (due to the capillary liquid holdup).[3,4]

In practice, commercial shaving foams fit perfectly in this range, and are expected to evolve mostly by coarsening, as a consequence of the small initial bubble size and low liquid fraction. To quantitatively check this behavior, we first measured the time evolution of the bubble size distribution, by

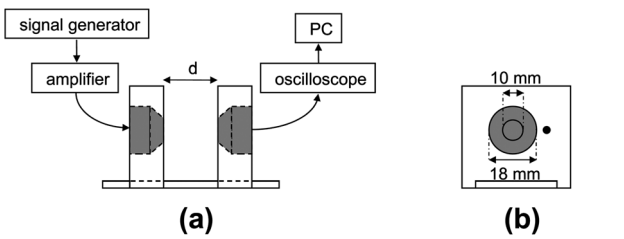

Fig. 1 Sketch of the experimental setup (not to scale). (a) Side view. The transducers are drawn in gray. The electrodes have not been represented. (b) Face view of the transducers. The electrode is represented by a black dot.

image analysis of samples of a coarsening commercial foam (Gillette) extracted at different times after its generation at $t = 0$, placed between two lamellae with spacers of controlled thickness and observed by a microscope. The evolution of the mean bubble radius $\langle a \rangle$ is shown in Fig. 2. It is in quantitative agreement with previous studies.[6] The bubble radius is multiplied by a factor 8 in 23 hours. We also measured a polydispersity index σ, defined as the ratio between the standard deviation and the mean of the bubble size distribution: $\sigma = \sqrt{\langle a^2 \rangle - \langle a \rangle^2}/\langle a \rangle$. Values of σ were scattered between 0.6 and 1.0, without any clear trend of evolution with the aging time.

In parallel, to estimate the evolution of the liquid fraction, we recorded the conductivity σ_f through the foam[14] using a pair of electrodes, inserted at the same height as the transducers (Fig. 1b). The signal is analyzed by a multiplexer (SR 715, Stanford Research Systems) and acquired on a computer *via* a home-made LabView program. We performed a reference experiment in the same geometry to measure the conductivity σ_ℓ of the liquid of the foaming solution alone. The relative conductivity $\sigma = \sigma_f/\sigma_\ell$ then gives the liquid fraction ϕ_ℓ, according to the phenomenological formula of Feitosa *et al.*:[14] $\phi_\ell = 3\sigma(1 + 11\sigma)/(1 + 25\sigma + 10\sigma^2)$. The corresponding curve is shown in Fig. 3. It shows a slow drainage behavior, namely the decrease of liquid fraction with time: ϕ_ℓ decreases by less than 33% in 17 hours. As a validation, our data are in quantitative agreement with previous measurements, which were obtained by a different technique (weighing).[29,40]

Consequently, with such commercial foams, the bubble size is slowly tuned, just by waiting, while the liquid fraction can be considered as almost constant. However, note that from one sample to another, we do not control perfectly the initial conditions; there is some random variation in initial liquid fraction profiles and bubble size distribution. More specifically, the inspection of the time evolution of the liquid fraction for different runs (data not shown) shows a variation of up to $\pm 15\%$ from the reference curve of Fig. 3.

For investigating the possible role of the chemical composition of the foam and the universality of the results, we

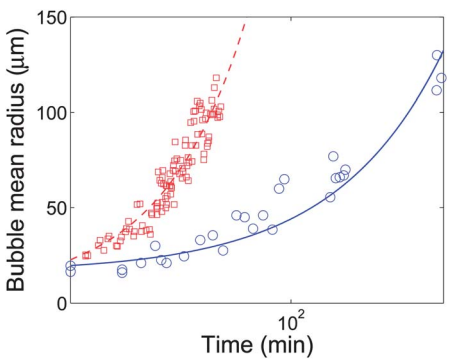

Fig. 2 Time evolution of the average bubble size of coarsening foams: Gillette shaving foam (○), and SDS foam with C_2F_6 (□). The lines are best fits of the data by a law $a = a_0 + \alpha t^\beta$, where if t is expressed in min: $a_0 = 16$ μm, $\alpha = 5.0$ S.I. and $\beta = 0.53$ for the Gillette foam; $a_0 = 5.2$ μm, $\alpha = 10.9$ S.I. and $\beta = 0.68$ for the SDS foam.

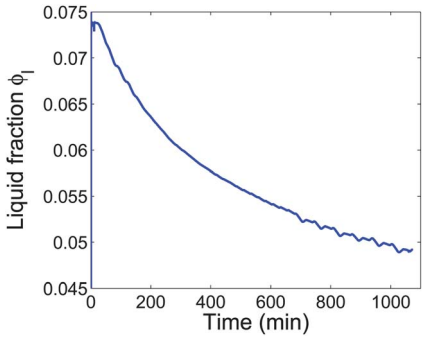

Fig. 3 Time evolution of the liquid fraction of coarsening shaving foam. The tiny oscillations at the very end of the curve are electronic artefacts.

performed complementary experiments on home-made foams, made from home-made solutions. These foams are made by a home-made double-syringe device, consisting of two plastic syringes, in which outlets are connected by a tube of inner diameter 2 mm and length 2 cm. Initially, to obtain any desired liquid fraction, a precise volume of surfactant solution is added in one of the syringes. The remaining volume is filled with the chosen gas. To produce the foam, the pistons of the syringes are alternatively actuated, forcing the gas–liquid mixture to circulate from one syringe to the other, and being strongly sheared within the connecting tube. For a solution of good foamability (like SDS), it requires about ten back and forth motions of the pistons to obtain an homogeneous and uniform foam, with an initial mean radius of 20 μm, and initial liquid fractions which can be chosen typically between 0.05 and 0.15.

With this device, we primarily tested solutions of sodium dodecyl sulfate (SDS) in ultrapure water at a concentration of 10 g L^{-1}. For further tests, we also used a solution of SLES (sodium lauryl ether sulfate) with co-surfactants (cocoylamidopropyl betaine and myristic acid), following the recipe given in ref. 35. In all cases, C_2F_6 is chosen for the gas, to adjust the coarsening dynamics, so that the coarsening times of the SDS- and SLES-based foams are suitably different from that of the Gillette shaving foams (Fig. 2).

C Selection of the insonation types and signal processing

A classical way to obtain the acoustic properties of a material is to send a pulse through it, and to measure the time of flight after which the pulse is received. It turns out that this seemingly straightforward method is not the most reliable in our case. First, the sharp pulse sent by the generator has a wide frequency spectrum, but our transducers are not broadband. Hence, they filter the pulse into a much longer and weaker signal. This blurs the start of the received signal, hence reduces the accuracy of measurement of the time of flight to at best 10^{-5} s; consequently, the uncertainty of this method to measure the speed of sound is at best 10%. In many cases, it is even impossible to extract precisely enough the start of the received signal from the background electronic noise. Second, there is an unknown impedance mismatch between the transducers and the foam. Hence, only part of the power delivered by the emitting

transducer is converted into an acoustic signal in the foam, and similarly only part of the acoustic wave impinging the receiving transducer is converted into an electric signal. Hence, it is not possible to deduce the attenuation length from the transmitted amplitude; it gives at best a qualitative estimate of how attenuation by the foam evolves with time. Another consequence of the impedance mismatch is a phase jump between the transducer and the foam, which affects the measurements of the time of flight. It is likely that there is a compensation of the phase jumps at the emitting and receiving transducers because of reciprocity, but it still may be a significant source of uncertainty in the speed of sound, since the time of flight is not much greater than the period of the signal, $1/f = 2.5 \times 10^{-5}$ s.

To overcome some of the limitations of the pulse method, we have preferentially chosen, for quantitative measurements, a continuous sinusoidal insonation at frequency f. We first checked whether the received signal is sinusoidal; therefore, we measured the phase difference and the amplitude ratio between the sent and received pulse. Since the transducers were used at different frequencies: 38, 40 and 42 kHz in some of our experiments (Section III A), we calibrated their frequency responses at these three frequencies, by placing them face to face at a given distance in air, sending a fixed sinusoidal signal, and measuring the received amplitude at 38, 40 and 42 kHz. The results shown in Section III A are corrected for this frequency response intrinsic to the transducer pair.

Mujica and Fauve[29] measured an attenuation length of the order of the wavelength, which is of order 1 mm. Hence, the signal is strongly attenuated over the distance between the transducers, which allows us to neglect multiple reflections. The phase difference thus obeys:

$$\varphi = \frac{2\pi d f}{c}. \quad (1)$$

Therefore, it is possible to measure the speed of sound from the dependence of the phase difference on the distance. The amplitude ratio between the sent and the received signals equals:

$$A = \frac{4ZZ_t}{(Z+Z_t)^2} e^{-\alpha d}, \quad (2)$$

where Z and Z_t are the acoustic impedances respectively of the foam and of the transducer, and α is the attenuation coefficient. Hence, it is possible to measure the attenuation coefficient from the dependence of the amplitude ratio on the distance.

III Experimental results

In this section, we first present detailed measurements on our selected combination: an aging Gillette shaving foam, studied in transmission, with a continuous insonation, and for various distances or frequencies (Section III A). Secondly, we report the results of similar experiments, but made on home-made foams (Section III B).

A Gillette shaving foams

We performed a series of experiments at a fixed frequency $f = 40$ kHz over about one day. At longer times, the foam dries up from its top, and the signals become irregular. We recorded the time evolution of the phase difference at the following distances: 5.0, 5.5, 6.0, 6.5 and 7.0 mm (Fig. 4).

At short times ($\lesssim 2 \times 10^2$ min), for each distance, the phase difference between the sent and the received signals increases, and the curves are approximately equally separated, in agreement with eqn (1). Fitting, at given times, the dependence of the phase difference on the distance by the linear law (1) yields a measurement of the speed of sound (Fig. 5): it decreases with time, but the evolution is slower and slower. Its order of magnitude is 50 m s^{-1}, in agreement with previous measurements.[29,34] However, the precision of this measurement decreases with increasing time, as the phase differences for different distances follow a different evolution.

By contrast, at long times ($\gtrsim 3 \times 10^2$ min), the phase difference shows a very slow decrease. The transition between this trend and the increase observed at short time is either rather smooth (at $d = 5.0$ and 7.0 mm) or characterized by a sharp decrease (at $d = 5.5$, 6.0 and 6.5 mm). We call the transition time the instant at which this transition occurs. After the transition time, it is not possible anymore to measure reliably the speed of sound from the dependence of the phase difference on the distance; however, the fact that the phase difference

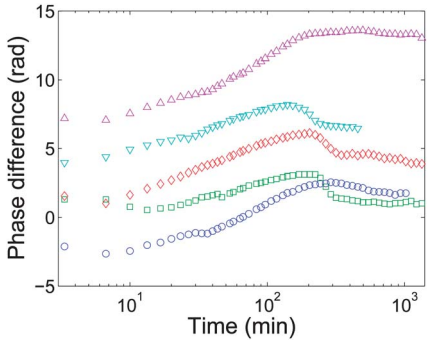

Fig. 4 Time evolution of the phase difference, for $d = 5.0$ (○), 5.5 (□), 6.0 (◇), 6.5 (▽) and 7.0 mm (△). The phase difference is measured except for an offset, similar for all data.

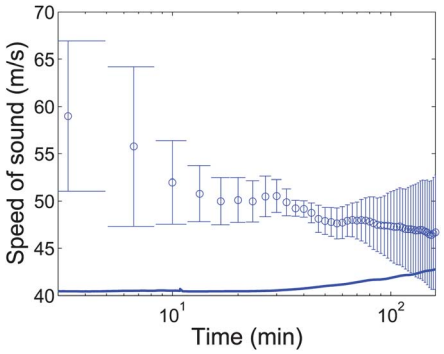

Fig. 5 Time evolution of the speed of sound. The circular symbols are experimental data; error bars come from the confidence interval on the best fit parameter of the fit of the data of Fig. 4 by (1). The line is the prediction by Wood's model (4), using the liquid fraction data of Fig. 3.

decreases, after its increase at short times, shows that the speed of sound passes through a minimum at the transition times and then increases.

The evolution of the amplitude ratio is shown in Fig. 6. At short times, for each distance, the amplitude ratio decreases. At long times, it reaches a plateau, at a value between 0.01 and 0.015. The overall time evolution is strongly correlated with that of the phase difference; notably, the experiments at $d = 5.5$, 6.0 and 6.5 mm show a marked minimum of amplitude ratio at intermediate times, simultaneously with the decrease of the phase difference. In contrast, the experiments at $d = 5.0$ and 7.0 mm show a faint minimum of transmission, consistent with the fact that the corresponding phase differences evolve smoothly (Fig. 4).

In practice, at short times, a clean analysis of the decrease of the amplitude ratio as a function of distance, in terms of the attenuation length, is difficult. Together with the differences between the curves at different distances, this is probably due to differences between the samples prepared for each experiment at a given distance. However, we can still extract a rough estimation of this length, which typically ranges from 3 cm^{-1} at the earliest ages to 10 cm^{-1} when approaching the minimum of amplitude.

We also performed an experiment at a fixed distance $d =$ 6 mm on a given coarsening foam, varying the frequency every 30 s. Our transducers being not broadband, we could only investigate a narrow range of frequencies, between 38 and 42 kHz, outside which the signal is too weak. The time evolution of the amplitude ratio is plotted for 38, 40 and 42 kHz in Fig. 7. At short times, the amplitude ratio decreases, and at long times, it reaches a plateau, consistent with the previous measurements (Fig. 6). The transition time is between 20 and 40 min, and increases with decreasing frequency.

B Complementary results on home-made foams

The features described previously are found for commercial shaving foams, having good ranges of variations of a and ϕ_ℓ, but these samples correspond to a given chemical composition (surfactant, polymers, additives). It is then crucial to check if similar properties are also found for other foams, with different, known and eventually more simple chemical formulation. We thus performed a series of experiments at a fixed frequency $f =$ 40 kHz on the SDS foams: it turns out that the overall trends are qualitatively similar to those of Gillette foams.

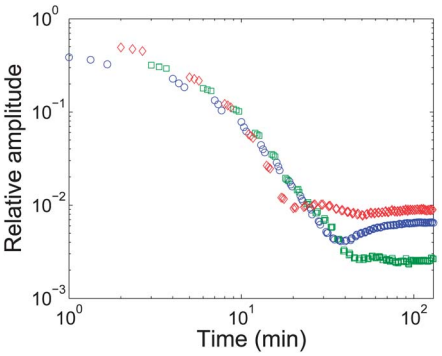

Fig. 7 Time evolution of the amplitude ratio, for $f = 38$ (□), 40 (○) and 42 kHz (◇).

At short times ($\lesssim$15 min), for each distance, the phase difference slowly increases, and the curves are approximately equally separated (Fig. 8). There is then a transition time around 15 min where the phase difference evolves more quickly, with a non-monotonous behavior (as seen for 1.4 and 1.8 mm). At longer times, the phase difference tends to plateau again.

In parallel, we also present the relative amplitude in Fig. 9. All curves show the same trend, similar to that of the shaving foams, with a pronounced minimum at a given transition time (here around 15 min, well corresponding to the transition time seen in the phase difference).

However, quantitatively, there are clear differences between the SDS foams and the shaving ones. First, we have found that, for SDS, the transition time is well below that of the shaving foams. This will be related in the following Discussion section, in terms of faster bubble diameter evolution for SDS foams (as seen in Fig. 2).

Secondly, the attenuation length is quite larger for SDS foams. In fact, we had to perform experiments at the following distances 1.2, 1.4, 1.6, 1.8 and 2.0 mm because the signal-to-noise ratio was not good enough at the larger distances used for

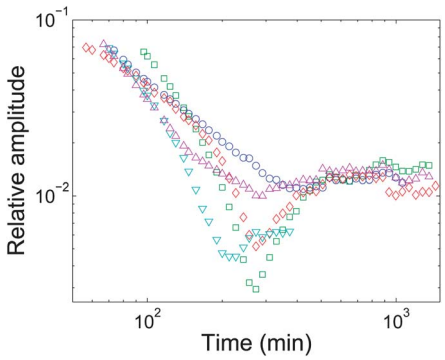

Fig. 6 Time evolution of the amplitude ratio, for $d = 5.0$ (○), 5.5 (□), 6.0 (◇), 6.5 (▽) and 7.0 mm (△). Data with amplitude ratio higher than 0.075 suffered from electronic distortion and are not shown.

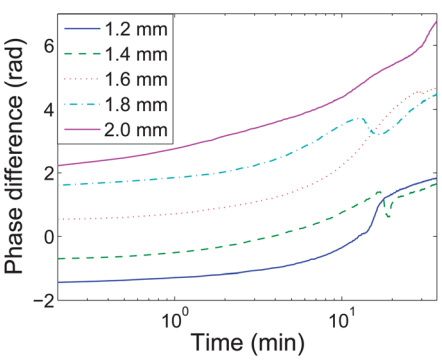

Fig. 8 Time evolution of the phase difference for the SDS foam, for $d = 1.2$, 1.4, 1.6, 1.8 and 2.0 mm. The phase difference is measured except for an offset, similar for all data.

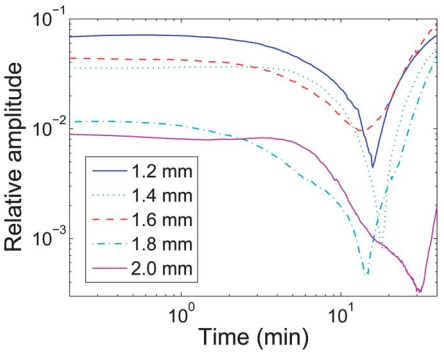

Fig. 9 Time evolution of the amplitude ratio for SDS foams, for $d = 1.2$, 1.4, 1.6, 1.8 and 2.0 mm.

shaving foams. For these distances, the curves are approximately equally separated in a logarithmic scale (with a better accuracy than for the shaving foams), and a reliable measurement of the attenuation can be obtained (eqn (2)). This attenuation length is finally of the order of magnitude 30 cm^{-1}, meaning that the signal is attenuated over a characteristic distance extremely short, of order 1 mm.

It turns out that the increase of the sound attenuation is indeed so strong with the SLES-based foams[35] that we could not get over the noise level, even at distances as short as 1 mm, preventing any possible measurements, and evidencing that these foams are the most absorbent of all we tested.

Lastly, as for the Gillette foam, we can use eqn (1) to deduce the evolution of the speed of sound at short times, before the evolutions at different distances become significantly different. Here again, the speed of sound decreases with time, in a way similar to that of the Gillette shaving foams. However, its order of magnitude is 25 m s^{-1}, about twice lower than that of shaving foams.

IV Discussion

A From transition times to a Minnaert-like resonance

As a robust trend, and for all the foam compositions, our experiments show a crossover between short-time and long-time behaviors, which can be quantified by a critical time (corresponding both to the minimum of transmission and sharp variation of the phase).

Time is indeed not the relevant parameter: as explained before, aging means increase of the bubble diameter. The liquid fraction evolves much slower than the bubble size and we will henceforth neglect its influence, see Section II B. So, our results suggest that the behavior of the acoustic properties is strongly dependent on the bubble size.

Fig. 2 gives an indication of the bubble radius at the transition time. For Gillette foams, at $t = 30$ min, it gives $a = 30$ μm, and at $t = 2 \times 10^2$ min, it gives $a = 60$ μm. For SDS foams, though the transition time is much shorter than for Gillette foams (15 min, as seen in Fig. 9), we find a similar value for the critical diameter, $a = 70$ μm (Fig. 2).

It is striking to find out that the different experiments always provided a critical radius in the same range, $a = 50 \pm 20$ μm, whatever the chemical formulation and transition time. The uncertainty in this critical radius is the consequence of the experimental uncertainties and variations in initial conditions (most likely a lack of control of the initial bubble size).

At this stage, it is tempting to invoke a resonance effect to explain the features occurring at this critical radius: for a given frequency, the bubbles become resonant, hence they pump a maximum of energy from the incident signal. It is well known that a single bubble in a liquid has a resonance frequency, called the Minnaert frequency:[15,16]

$$\omega_0^2 = \frac{3\gamma P_0}{\rho_w a^2}, \tag{3}$$

where $\gamma = 1.1$ is the ratio of specific heats of the gas at constant pressure and constant volume,[29] $P_0 = 10^5$ Pa is the ambient pressure, $\rho_w = 10^3$ kg m^{-3} is the liquid density and a is the bubble radius. Bubbly liquids (at gas volume fraction lower than 1%) show a maximum of attenuation and a minimum of speed of sound, when the Minnaert criterion is fulfilled.[20,21]

The Minnaert criterion (3) yields a bubble radius of 72 μm at the resonance for the frequency of 40 kHz, which is surprisingly close to the critical bubble radius found here in the foams. However, the Minnaert frequency stands for a single bubble in an unbound liquid, whose density is much higher than that of a foam. In this respect, it is not expected to be suited for close-packed bubbles.

At this stage, we can make a few remarks. First, it is worth noting that such an unexpected agreement with the Minnaert frequency has been reported in the context of the sound emitted by bubble popping at the surface of a foam,[41] but also remains theoretically unexplained in these cases. Secondly, using the foam density instead of that of pure water in (3) leads to an increase of the resonance radius by a factor 4, hence to a resonance radius of 300 μm at 40 kHz, which clearly differs from the experiments.

Also, note that the previous studies have not reported such a resonance-like behavior.[29,34] We believe that a possibly important difference is that the sample is not confined in a closed box in our experiments, but open to the air. This experimental configuration increases the coarsening rate, allowing us to reach larger bubble sizes over similar aging times, and—together with longer experimental runs—to finally have access to the resonance effects. For the Gillette and C_2F_6 foams studied here, the coarsening rate is faster because the outside gas (air) actually diffuses into these foams. This is a known effect, when dealing with different inside/outside gases, which can lead to significant foam expansion and rapid bubble coarsening, especially when the outside gas is the most soluble in water (as in our case).[42]

It is thus difficult to be more conclusive in these comparisons to previous studies, since the aforementioned studies did not report the evolution of the bubble size during their own experiments, and since aging time is not the relevant parameter (as explained before). Nevertheless, on other quantitative aspects, we still found a good agreement with previous studies, like for the speed of sound in shaving foams; also, the attenuation lengths are similar.

Lastly, although our data show that the occurrence of the resonance at a given radius (set by the frequency) is robust and independent of the foam composition and aging timescale, our data also show that all the acoustic properties of these foams are not equal. In particular, there is a clear dependence of the attenuation length on the chemicals. On this issue, it seems reasonable that the addition of co-surfactant to the simple SLES solution leads to stronger attenuation. This is consistent with the known fact that the co-surfactants used here drastically increase the interfacial viscosity of the bubbles,[35] thereby providing an extra source of dissipation of the sound. In this respect, it is thus finally surprising to find that the shaving foams (having the more complex formulation) are less dissipative of all these foams.

B Comparison of the measurements with models

From the previous stage of data analysis, we have found that an acoustic resonance effect occurs in aqueous foams, and have drawn some links with Minnaert's prediction for the resonance of a single bubble. However, as already stated, the crudest approach consisting of replacing the liquid density in the one-bubble Minnaert model by the effective foam density is not in agreement with the data. We thus have to consider more complex models of sound propagation in a bubbly medium, and compare them to our data.

First, note that, for the shaving foams, the acoustic wavelength, $\lambda = c/f \simeq 1.3$ mm, is at least one order of magnitude larger than the bubble radius (at early times and up to the critical radius). In that limit $\lambda \gg R$, a simple model of sound in foams, called Wood's model,[36] has been proposed, stating that the acoustic propagation probes an effective medium with average density $\langle\rho\rangle = (1-\phi_\ell)\rho_g + \phi_\ell\rho_w$ and compressibility $\langle\chi\rangle = (1-\phi_\ell)\chi_g + \phi_\ell\chi_w$, where the subscripts g and w denote gas and water; hence, $c = 1/\sqrt{\langle\rho\rangle\langle\chi\rangle}$. Since $\rho_g \ll \rho_w$ and $\chi_g \gg \chi_w$, the speed of sound is approximately:

$$c_{\mathrm{Wood}} \simeq \frac{1}{\sqrt{\rho_w\chi_g\phi_\ell(1-\phi_\ell)}}. \quad (4)$$

Using the measurements of the liquid fraction (Fig. 3), we superimpose the prediction of the speed of sound given by Wood's model on the experimental measurements, as shown in Fig. 5. Like previous studies,[27,29] we find that Wood's model underestimates the speed of sound. But there is a first qualitative discrepancy: since the liquid fraction decreases owing to drainage, Wood's model predicts an increase of the speed of sound with time, whereas in experiments it decreases at short times. The main limitation of Wood's model is that it is a mean field approach, and it does not take into account bubble-scale effects, like the Minnaert resonance of each bubble.

To implement Wood's model, Mujica and Fauve[29] adapted Biot's phenomenological poroelastic model to foams, and accounted for the network elasticity conferred by the Gibbs elasticity of the gas/liquid interfaces. They found a correction to Wood's model of the form $c = c_{\mathrm{Wood}}(1+\phi_\ell\chi_g K_b)$, with a network elastic modulus scaling as $K_b \propto 1/\langle a\rangle$, see eqn (28) in ref. 29. However, this correction still yields a very smooth evolution of the speed of sound with time, which cannot capture the sharp evolution of the phase difference (Fig. 4) or amplitude. Furthermore, this network correction is based on the unrealistic assumption that every bubble is surrounded by a water shell of constant effective thickness, while bubbles in a foam are surrounded by both thick plateau borders and thin facets (the latter ones covering $\approx$75% of the bubble area in the dry foam), whose thickness differs by several orders of magnitude.

Beside mean-field and phenomenological models, many other models have been proposed for calculating the effective wavenumber in a complex medium. In the following, we focus on Foldy's model[43] and its extension by Waterman and Truell.[44] The reason for this choice is that Foldy's model was found to be efficient for describing bubbly liquids,[20] and even when resonant effects were strong.[21] However, Foldy's model is limited to dilute systems, making it inapplicable to foams, in particular because it does not consider the change of the density due to the scatterers. In 1962, Waterman and Truell proposed an improved model, in which the effective wavenumber k is given by:

$$k^2 = \left(k_0^2 + 4\pi n f_0\right)\left(1 + \frac{4\pi n f_1}{k_0^2}\right), \quad (5)$$

where k_0 is the wavenumber in the host medium, n the number of scatterers per unit volume, and f_0 and f_1 the scattering functions for the monopolar and dipolar modes, respectively. Interestingly, it can be shown that each mode has a different contribution: the monopolar mode dictates the effective compressibility of the medium, whereas the dipolar mode gives the effective density. In our case, the monopolar and dipolar modes are associated respectively with the volumetric oscillations and with the translation of the bubbles. For bubbles of radius a and of density n in water, eqn (5) becomes:

$$k^2 = \omega^2\left[\chi_w + 4\pi n\,\frac{a\left(1-\omega_0^2\rho_w\chi_w a^2/3\right)}{\omega_0^2 - \omega^2(1-\mathrm{i}\delta)}\right]\left[\rho_w + \frac{4}{3}\pi n a^3\left(\rho_g - \rho_w\right)\right], \quad (6)$$

where δ is the damping constant for the oscillations of a single bubble.[16] Note that Wood's approximation is recovered if the frequency is well below the Minnaert frequency. For a polydisperse system, n needs to be replaced by $\int n(a)\mathrm{d}a$ where $n(a)\mathrm{d}a$ is the number of bubbles per unit volume whose radius is between a and $a + \mathrm{d}a$. For foams, the size distribution is well described by a log-normal law:

$$n(a) = \frac{n_{\mathrm{tot}}}{a\varepsilon\sqrt{2\pi}}\exp\left[-\frac{\left(\ln(a/a_0)\right)^2}{2\varepsilon^2}\right], \quad (7)$$

where n_{tot} is the total number of bubbles per unit volume, a_0 the median radius, and ε the log-normal standard deviation. The mean radius $\langle a\rangle$ and the normalized standard deviation $\sigma = \sqrt{\langle\left(a/\langle a\rangle - 1\right)^2\rangle}$ are related to a_0 and ε by the following relationships: $a_0 = \langle a\rangle \mathrm{e}^{-\varepsilon^2/2}$ and $\varepsilon = \sqrt{\ln(1+\sigma^2)}$.

We report in Fig. 10 the prediction of eqn (6) for the attenuation and phase velocity at 40 kHz in a $\phi_\ell = 6\%$ foam, as functions of the mean radius of bubbles. We consider the two

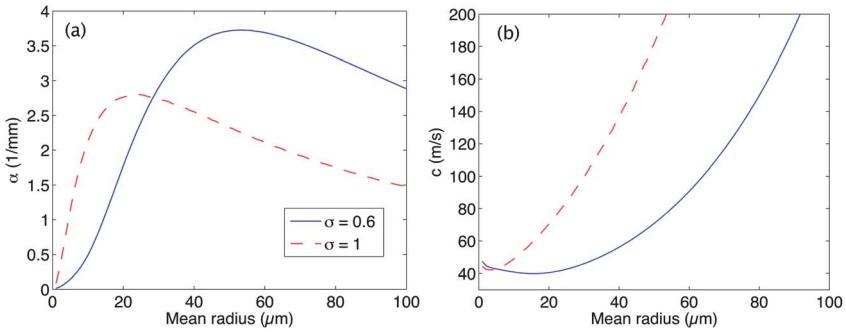

Fig. 10 Prediction of Waterman and Truell's model for the effective wavenumber at 40 kHz in a 94% dispersion of air bubbles in water as a function of the mean radius of the bubbles: (a) attenuation $\alpha = \mathrm{Im}(k)$; (b) phase velocity $c = \omega/\mathrm{Re}(k)$. Two polydispersities are considered: $\sigma = 0.6$ (solid line) and $\sigma = 1$ (dashed line).

extreme values of the measured polydispersity, $\sigma = 0.6$ and 1.0 (see Section II B). Note that we take the simple case of air bubbles in water, even though Gillette foams are composed of different gases and liquids. We have checked that the orders of magnitude of α and c were not modified by changes in parameters such as the viscosity of the fluid or the thermal diffusion constant of the gas.

The attenuation curve (Fig. 10a) shows a maximum for a mean radius close to the Minnaert radius. Its shape for $\sigma = 0.6$ is consistent with the measured transmitted amplitude in Fig. 6. However, the qualitative agreement is not good: with $\alpha = 3\ \mathrm{mm}^{-1}$, the transmitted signal through 6 mm would be of the order of 10^{-8}, well below the minimal signal we can detect with our setup. The influence of polydispersity is far from negligible: the maximum of attenuation is not reached for the same mean radius when σ changes, which could explain why the transition time changes from one experiment to the other.

The predicted phase velocity (Fig. 10b) also shares some common features with the experimental observations. The decrease followed by an increase is predicted. However, because of the high level of polydispersity, the minimum of velocity is not reached for the Minnaert radius, but for a smaller radius. Note that, as Wood's model, Waterman and Truell's model predicts a smaller phase velocity ($\simeq 40\ \mathrm{m\ s}^{-1}$) than what is measured for small mean radii ($\simeq 50\ \mathrm{m\ s}^{-1}$). The high values of c in Fig. 10 for very small radii are due to surface tension effects and correspond to 1 μm radius bubbles, which are not present in our foams (the smallest mean radii are around 15 μm according to Fig. 2).

The discrepancy between Waterman and Truell's model and our experimental measurements is not a surprise, because this model is based on the assumption that scattering events are independent. It means that correlations between the positions of the scatterers and loops (*i.e.* scattering paths visiting several times the same scatterer) are neglected. For such close-packed systems as foams, these two types of events may be significant, especially if resonances exist. More sophisticated models that include loops[45,46] or correlations[47] might give better agreement. The Coherent Potential Approximation (CPA),[48,49] for instance, gives good predictions for close-packed systems.[50] However, it is remarkable to observe that the simple eqn (6) already gives an insight on the acoustic properties of aqueous foams; in particular, it predicts the observed non-monotonous evolutions of the speed of sound and attenuation.

V Summary and conclusions

We have collected a large set of new data on how sound propagates through an aqueous foam (in the frequency range of 40 kHz). First, as previously observed, our measurements show how different is the acoustics of a foam when compared to the sound propagation through a pure liquid or through a pure gas. Clearly, by dispersing gas bubbles in a fluid, one gets a very peculiar material, acoustically speaking.

We also definitively show here that mean-field approaches, based on effective or averaged quantities, are too simplistic to describe the acoustic of foams. Our results actually prove that one must take into account the mesoscopic scale of the bubble and the complex spatial distribution of gas and liquid at this scale. Indeed, this is fully illustrated by the original observation of resonance-like features, occurring at a critical bubble size. It is worth noting that the existence of this resonance—really constituting an important breakthrough in foam acoustics—is seen in all types of foams we studied, whatever be the mode of insonation, and in all the measured acoustic quantities.

At this stage, it is tempting to link these results to the Minnaert single-bubble resonance, though it is surprising to find reminiscence of this effect within the collection of packed bubbles. As we have discussed in detail in this article, by adapting the existing models to foams, we can actually predict some qualitative trends, consistent with the resonance and data, but there remains a quantitative gap between these data and the model predictions. Further studies are thus clearly needed on these theoretical aspects.

In parallel, more experimental work is also needed. First, experiments will have to be performed with an optimized acoustic setup, and various controlled bulk and interfacial viscoelasticities. More importantly, these new results, evidencing some sample reproducibility issues, show that highly controlled foams are crucially required, in terms of controlled polydispersity, liquid fraction and uniformity. Compared to studies on other foam properties, it seems that unraveling how sound propagates in a foam first requires a much higher level of sample control. Inverting the problem, we

can then expect in the future, with an acoustic diagnostic, to characterize a foam (or other types of dispersions) in much more detail than with other techniques.

Acknowledgements

The authors thank Florence Elias for initial discussion and experimental tests, and the Agence Nationale de la Recherche for the financial support (project number: ANR-11-BS09).

References

1 R. K. Prud'homme and S. A. Khan, *Foams: Theory, Measurements, and Applications*, Marcel Dekker Inc., New York, 1997.
2 A. Saint-Jalmes, D. J. Durian, D. A. Weitz, *Foams, in Kirk-Othmer Encyclopedia of Chemical Technology*, 5th edn, 2005.
3 I. Cantat, S. Cohen-Addad, F. Elias, F. Graner, R. Höhler, O. Pitois, F. Rouyer, A. Saint-Jalmes, *Les mousses, structure et dynamique*, Belin, Paris, 2010.
4 A. Saint-Jalmes, *Soft Matter*, 2006, **2**, 836.
5 D. J. Pine, D. A. Weitz, P. M. Chaikin and E. Herbolzheimer, *Phys. Rev. Lett.*, 1988, **60**, 1134.
6 D. J. Durian, D. A. Weitz and D. J. Pine, *Phys. Rev. A: At., Mol., Opt. Phys.*, 1991, **44**, R7902.
7 D. A. Weitz, D. J. Pine, in *Dynamic Light Scattering: the Methods and Applications*, Oxford University Press, Oxford, 1993, p. 652.
8 M. U. Vera and D. J. Durian, *Phys. Rev. E: Stat. Phys., Plasmas, Fluids, Relat. Interdiscip. Top.*, 1996, **53**, 3215.
9 M. U. Vera, A. Saint-Jalmes and D. J. Durian, *Appl. Opt.*, 2001, **40**, 4210.
10 J. Lambert, R. Mokso, I. Cantat, P. Cloetens, J. A. Glazier, F. Graner and R. Delannay, *Phys. Rev. Lett.*, 2010, **104**, 238404.
11 N. O. Clark, *Trans. Faraday Soc.*, 1948, **44**, 13.
12 A. K. Datye and R. Lemlich, *Int. J. Multiphase Flow*, 1983, **9**, 627.
13 R. Phelan, D. Weaire, E. A. J. F. Peters and G. Verbist, *J. Phys.: Condens. Matter*, 1996, **8**, L475.
14 K. Feitosa, S. Marze, A. Saint-Jalmes and D. J. Durian, *J. Phys.: Condens. Matter*, 2005, **17**, 6301.
15 M. Minnaert, *Philos. Mag.*, 1933, **16**, 235.
16 T. G. Leighton, *The Acoustic Bubble*, Academic Press, San Diego, 1994.
17 M. Devaud, T. Hocquet, J. C. Bacri and V. Leroy, *Eur. J. Phys.*, 2008, **29**, 1263.
18 D. Rabaud, P. Thibault, M. Mathieu and P. Marmottant, *Phys. Rev. Lett.*, 2011, **106**, 134501.
19 D. Rabaud, P. Thibault, J. P. Raven, O. Hugon, E. Lacot and P. Marmottant, *Phys. Fluids*, 2011, **23**, 042003.
20 K. W. Commander and A. Prosperetti, *J. Acoust. Soc. Am.*, 1989, **85**, 732.
21 V. Leroy, A. Strybulevych, J. H. Page and M. G. Scanlon, *J. Acoust. Soc. Am.*, 2008, **123**, 1931.
22 M. Nicholas, R. A. Roy, L. A. Crum, H. Oğuz and A. Prosperetti, *J. Acoust. Soc. Am.*, 1994, **95**, 3171.
23 P. A. Hwang, R. A. Roy and L. A. Crum, *J. Atmos. Oceanic Tech.*, 1995, **12**, 1287.
24 P. A. Hwang and W. J. Teague, *J. Atmos. Oceanic Tech.*, 2000, **17**, 847.
25 A. Bretagne, A. Tourin and V. Leroy, *Appl. Phys. Lett.*, 2011, **99**, 221906.
26 N. T. Moxon, A. C. Torrance and S. B. Richardson, *Appl. Acoust.*, 1988, **24**, 193.
27 I. I. Goldfarb, I. R. Shreiber and F. I. Vafina, *J. Acoust. Soc. Am.*, 1992, **92**, 2756.
28 I. Goldfarb, Z. Orenbach, I. Schreiber and F. Vafina, *Shock Waves*, 1997, **7**, 77.
29 N. Mujica and S. Fauve, *Phys. Rev. E: Stat., Nonlinear, Soft Matter Phys.*, 2002, **66**, 021404.
30 K. B. Kann and A. A. Kislitsyn, *Colloid J.*, 2003, **65**, 31.
31 K. B. Kann, *Colloids Surf., A*, 2005, **263**, 315.
32 A. Britan, M. Livers and G. Ben-Dor, *Colloids Surf., A*, 2009, **344**, 48.
33 M. Erpelding, R. M. Guillermic, B. Dollet, A. Saint-Jalmes and J. Crassous, *Phys. Rev. E: Stat., Nonlinear, Soft Matter Phys.*, 2010, **82**, 021409.
34 D. Daugelaite, Time Dependent Studies of Foam Stability Using Image Analysis, Electrical Resistivity and Ultrasound, PhD thesis, University of Manitoba, 2011.
35 K. Golemanov, N. D. Denkov, S. Tcholakova, M. Vethamuthu and A. Lips, *Langmuir*, 2008, **24**, 9956.
36 A. B. Wood, *A Textbook of Sound*, Bell and Sons, London, 1944.
37 M. L. Cowan, I. P. Jones, J. H. Page and D. A. Weitz, *Phys. Rev. E: Stat., Nonlinear, Soft Matter Phys.*, 2002, **65**, 066605.
38 J. H. Page, M. L. Cowan, D. A. Weitz, B. A. van Tiggelen, Diffusing Acoustic Wave Spectroscopy: Field Fluctuation Spectroscopy with Multiply Scattered Ultrasonic Waves, in *Wave Scattering in Complex Media: From Theory to Applications*, ed. B. A. van Tiggelen and S. Skipetrov, Kluwer Academic Publishers, NATO Science series, Amsterdam, 2003, vol. 151.
39 V. Leroy, A. Bretagne, M. Fink, H. Willaime, P. Tabeling and A. Tourin, *Appl. Phys. Lett.*, 2009, **95**, 171904.
40 H. Hoballah, R. Höhler and S. Cohen-Addad, *J. Phys. II*, 1997, **7**, 1215.
41 J. Ding, F. W. Tsaur, A. Lips and A. Akay, *Phys. Rev. E: Stat., Nonlinear, Soft Matter Phys.*, 2007, **75**, 041601.
42 G. Maurdev, A. Saint-Jalmes and D. Langevin, *J. Colloid Interface Sci.*, 2006, **300**, 735.
43 L. L. Foldy, *Phys. Rev.*, 1945, **67**, 107.
44 P. C. Waterman and R. Truell, *J. Math. Phys.*, 1961, **2**, 512.
45 S. G. Kargl, *J. Acoust. Soc. Am.*, 2002, **111**, 168.
46 F. S. Henyey, *J. Acoust. Soc. Am.*, 1999, **105**, 2149.
47 J. Keller, *Stochastic Equations and Wave Propagation in Random Media, Proc. Symp. Appl. Math.*, Am. Math. Soc., McGraw-Hill, New York, 1964, vol. 16, pp. 145–170.
48 P. Sheng, *Introduction to Wave Scattering, Localization and Mesoscopic Phenomena*, Springer, Heidelberg, 2nd edn, 2006.
49 C. M. Soukoulis, S. Datta and E. N. Economou, *Phys. Rev. B: Solid State*, 1994, **49**, 3800.
50 J. H. Page, P. Sheng, H. P. Schriemer, I. Jones, X. Jing and D. A. Weitz, *Science*, 1996, **271**, 634.

